THE JOURNAL OF COMPARATIVE NEUROLOGY 469:325–339 (2004)

Neurogenesis and Stereological Morphometry of Calretinin-Immunoreactive GABAergic Interneurons of the Neostriatum

VLADIMIR V. RYMAR, RACHEL SASSEVILLE, KELVIN C. LUK, AND ABBAS F. SADIKOT*
Department of Neurology and Neurosurgery, Montreal Neurological Institute, McGill University, Montreal, Quebec H3A 2B4, Canada

ABSTRACT

We determined the neurogenesis characteristics of a distinct subclass of rat striatum γ-aminobutyric acidergic (GABAergic) interneurons expressing the calcium-binding protein calretinin (CR). Timed-pregnant rats were given an intraperitoneal injection of 5-bromo-2′-deoxyuridine (BrdU), a marker of cell proliferation, on designated days between embryonic day 12 (E12) and E21. CR-immunoreactive (-IR) neurons and BrdU-positive nuclei were labeled in the adult neostriatum by double immunohistochemistry, and the proportion of double-labeled cells was quantified. CR-IR interneurons of the neostriatum show maximum birth rates (>10% double labeling) between E14 and E17, with a peak at E15. CR-IR interneurons occupying the lateral half of the neostriatum become postmitotic prior to medial neurons. In the precomissural neostriatum, the earliest-born neurons occupy the lateral quadrants and the latest-born neurons occupy the dorsomedial sector. No significant rostrocaudal neurogenesis gradient is observed. CR-IR neurons make up 0.5% of the striatal population and are localized in both the patch and the matrix compartments. CR-IR neurons of the patch compartment are born early (E13–15), with later-born neurons (E16–18) populating mainly the matrix compartment. CR-IR cells of the neostriatum are a distinct subclass of interneurons that are born at an intermediate time during striatal development and share common neurogenesis characteristics with other interneurons and projection neurons produced in the ventral telencephalon. J. Comp. Neurol. 469:325–339, 2004.

Indexing terms: basal ganglia; caudate-putamen; bromodeoxyuridine; calcium-binding proteins; development; patch-matrix

The neostriatum receives massive glutamatergic inputs from the cerebral cortex and thalamus and monoaminergic afferents from the brainstem (Parent, 1996; Kawaguchi, 1997). Striatal efferents to the pallidal segments and to the midbrain arise from medium-sized γ-aminobutyric acidergic (GABAergic) spiny cells, which make up over 90% of striatal neurons (Kemp and Powell, 1971; Grofova, 1975; Somogyi and Smith, 1979). Less numerous aspiny interneurons receive inputs from striatal afferents and other striatal neurons. Interneurons play an important regulatory role in the activity of spiny projection neurons (Lapper and Bolam, 1992; Lapper et al., 1992; Kawaguchi, 1997; Rudkin and Sadikot, 1999; Sidibé and Smith, 1999). Four largely nonoverlapping classes of striatal interneurons are immunohistochemically identified: 1) large cholinergic neurons (Butcher and Hodge, 1976; Bolam et al., 1984); 2) a class of GABAergic neurons that colocalize nitric oxide synthase (NOS), somastostatin (SS), and neuropeptide Y (NPY; DiFiglia and Aronin, 1982; Vincent and Johansson, 1983); 3) GABAergic neurons that contain the calcium binding protein parvalbumin (PV; Gerfen et al., 1985; Cowan et al., 1990); 4) and GABAergic neurons that

Grant sponsor: Canadian Institutes of Health Research; Grant number: MOP53281; Grant sponsor: Parkinson Society of Canada; studentship; Grant sponsor: March of Dimes Birth Defects Foundation; Grant number: 1FY02-14; Grant sponsor: Fonds de la recherche en santé du Quebec (FRSQ) (V.V.R.); Grant sponsor: Montreal Neurological Institute Preston-Robb Fellowship (V.V.R.); Grant sponsor: FRSQ Senior Investigator Award (A.F.S.).

*Correspondence to: Abbas F. Sadikot, Cone Laboratory for Research in Neurosurgery, Montreal Neurological Institute, Room 109A, 3801 University St., Montreal, Quebec H3A 2B4, Canada. E-mail: sadikot@bic.mni.mcgill.ca

Received 13 May 2003; Revised 5 September 2003; Accepted 9 September 2003
DOI 10.1002/cne.11008
Published online the week of January 5, 2004 in Wiley InterScience (www.interscience.wiley.com).

contain the calcium binding protein calretinin (CR; Jacobowitz and Winsky, 1991; Résibois and Rogers, 1992; Bennett and Bolam, 1993; Kubota et al., 1993; Figueredo-Cardenas et al., 1996; Sadikot et al., 1996).

The neurogenesis timetable of striatal neurons is derived from earlier [^{3}H]thymidine autoradiography studies and more recent studies using an immunohistochemical method based on nuclear incorporation of the thymidine analog, 5-bromo-2′-deoxyuridine (BrdU). In the rat, striatal projection neurons are born over an extended period between E13 and E22, with peak neurogenesis at E15–18 (Fentress et al., 1981; Bayer, 1984; Marchand and Lajoie, 1986). Cholinergic interneurons are born early, between E12 and E15 (Semba et al., 1988; Phelps et al., 1989). PV-IR (Sadikot and Sasseville, 1997) and SS-IR interneurons (Semba et al., 1988) of the neostriatum are generated mainly between E14 and E17, with peak neurogenesis at E15–16. Spatial gradients of neurogenesis can also be identified. Cholinergic and PV-IR interneurons show prominent caudorostral gradients of neurogenesis (Semba et al., 1988; Phelps et al., 1989; Sadikot and Sasseville, 1997). SS-IR interneurons, on the other hand, show no apparent spatial neurogenesis gradient in the striatum (Semba et al., 1988). Neurogenesis gradients of neostriatum projection neurons are complex and depend on the rostrocaudal position of neurons in relationship to the anterior commissure (Bayer, 1984; Marchand and Lajoie, 1986). Neuronal birth date varies with respect to the chemically heterogeneous patch-matrix compartments of the striatum (Marchand and Lajoie, 1986; van der Kooy and Fishell, 1987; Song and Harlan, 1994). Spiny projection neurons that occupy the patch become postmitotic early, whereas later-born neurons occupy mainly the matrix compartment. In the case of interneurons, cholinergic cells destined for patch compartments are born earlier than those occupying the matrix (van Vulpen and van der Kooy, 1998). Whether this pattern of distinct neuronal birth dates within patch-matrix compartments applies to GABAergic interneurons is unknown.

In the present study, we determined the temporal and spatial neurogenesis gradients of CR-IR GABAergic neostriatal interneurons. We used an immunohistochemical method based on BrdU incorporation by dividing cells (Nowakowski et al., 1989), combined with labeling for chemospecific phenotypic markers in central nervous system tissue (del Rio and Soriano, 1989). We have previously characterized the neurogenesis of striatal PV-IR interneurons with a similar double-labeling method (Sadikot and Sasseville, 1997). Here we also analyzed the morphology of CR-IR neurons, including an unbiased estimate of cell number obtained from stereology. Finally, we characterized the distribution of CR-IR with respect to the chemically heterogeneous striatal patch-matrix compartments (Graybiel and Ragsdale, 1978; Herkenham and Pert, 1981) and determined differences in birth date of CR-IR neurons occupying either compartment. This work has previously been published in abstract form (Rymar and Sadikot, 2001, 2002).

MATERIALS AND METHODS

Experimental animals

Female rats (Sprague-Dawley, Charles River, LaSalle, Quebec, Canada) were coupled with males between 4 PM and 6 PM. The first 24 hr after coupling was designated as *embryonic day 0* (E0). Dams received a single intraperitoneal (i.p.) injection of BrdU (Sigma, St. Louis, MO; 50 mg/kg, in Tris-buffered saline, pH 7.6) at 5 PM at the onset of E12–21. Three dams were injected at each designated day, for a total of 30 animals. All animals were given food and water ad libitum. Litters were culled to 10 pups per dam at birth, and animals were weaned at 3 weeks after birth. Five males were selected from each litter and processed for immunohistochemistry between postnatal day 35 (P35) and P42. Seven additional animals of the same age were used for unbiased stereological estimates of neuronal number and quantification of cell size.

Animals were deeply anesthetized by using an overdose of sodium pentobarbital (75 mg/kg, i.p.) and perfused transcardially with an initial wash of heparinized 0.9% saline (50–100 ml, 4°C), followed by 4% paraformaldehyde in phosphate buffer (300 ml, 0.1 M, pH 7.4, 4°C). Brains were immersed for 48 hours in 30% phosphate-buffered sucrose solution (pH 7.4) and then cut in the coronal plane at 50 μm on a sliding freezing microtome. Free-floating sections were collected in phosphate-buffered saline (PBS; 0.1 M, pH 7.4) as separate sets so that each set contained every sixth serial section. Selected adjacent free-floating sections were processed for double-labeling immunohistochemistry for BrdU and CR, BrdU and calbindin (CB), or only CR, then mounted on glass slides, dehydrated, and coverslipped.

Immunohistochemistry

BrdU immunohistochemistry was performed by using minor modifications of a previously published method (Soriano and del Rio, 1991; Sadikot and Sasseville, 1997). Sections were incubated in 0.5% sodium borohydride dissolved in PBS for 20 minutes and rinsed twice in PBS. Next, sections were incubated for 30 minutes in 1% Triton X-100 in PBS containing 0.03% hydrogen peroxide, followed by 1% dimethlysulfoxide (DMSO) in PBS for 10 minutes. Sections were immersed in 2 N HCl in PBS for 60 minutes, then neutralized by rinsing in sodium borate buffer (0.1 M, pH 8.5) for 5 minutes. After brief washes in PBS (3 × 5 minutes), sections were preincubated in PBS containing 10% bovine serum albumin (BSA) and 0.3% Triton X-100 for 30 minutes, briefly rinsed in PBS, and then incubated for 14–16 hours in PBS containing mouse anti-BrdU antibody (1:40; Becton-Dickinson, San Jose, CA) and 2% BSA (4°C). After three brief rinses in PBS, sections were incubated in PBS containing secondary antibody (biotinylated antimouse IgG; 1:200; Vector, Burlingame, CA) and 2% BSA. After three brief rinses in PBS, sections were incubated for 1 hour in avidin-biotin complex (ABC; 1%, in PBS; Vector). Next, sections were briefly rinsed three times in PBS, and the immunohistochemical reaction product was revealed by incubation for 7–10 minutes in a solution containing 0.37 g nickel ammonium sulfate, 25 mg 3.3′-diaminobenzidine tetrahydrochloride (DAB), and 2 μl hydrogen peroxide (30%) dissolved in 100 ml Tris buffer (0.05 M, pH 7.6). This nickel-enhanced DAB-based chromogen yields a blue-black reaction product. Sections were thoroughly rinsed in PBS and then mounted out of distilled water on glass slides or prepared for immunohistochemistry for the second antigen.

For double immunohistochemistry, sections were incubated for 14–16 hours at room temperature in PBS containing a rabbit anti-CR antibody (1:5,000; Swant). After

three brief rinses in PBS (3 × 5 minutes each), sections were incubated for 1 hour in PBS containing secondary antibody (biotinylated anti-rabbit IgG; 1:200; Vector) and 2% BSA. After three rinses in PBS, sections were incubated in ABC (1%, in PBS). A light brown immunohistochemical reaction product was obtained by using a solution containing 25 mg DAB, 1% imidazole (1.0 M), and 20 μl hydrogen peroxide (30%) dissolved in Tris buffer (0.05 M, pH 7.6). After 10–15 minutes of exposure to the DAB chromogen, sections were rinsed thoroughly with PBS. Sections were mounted out of distilled water, air dried, dehydrated in a graded series of alcohols, cleared in Xylene Substitute (Shandon, Pittsburgh, PA), and coverslipped with Permount (Fisher, Fair Lawn, NJ). As control experiments, we omitted either anti-CR or anti-BrdU from the immunostaining schedule and noted no evidence of cross-reactivity. Furthermore, BrdU immunostaining was clearly nuclear, whereas anti-CR recognized cell bodies and processes. We also determined the number of striatal CR-IR neurons in BrdU/CR double-labeled sections and in sections from the same animals immunostained for CR only and found similar results. Finally, we used unbiased stereology to compare the number of CR-IR neurons in offspring of animals injected with BrdU and in animals not injected with BrdU, obtaining similar neuron numbers, indicating that BrdU itself is not toxic to striatal CR-IR neurons at the dose used in these experiments.

To determine whether subpopulations of neostriatum CR-IR neurons were cholinergic, sections from nine animals were processed for double immunofluorescence for CR and choline acetyltransferase (ChAT). Free-floating sections were incubated in TBS (0.1 M Tris, 1.4% NaCl, pH 7.3) containing primary antibodies against CR (rabbit anti-CR; 1:5,000; Swant) and ChAT (monoclonal mouse anti-ChAT; 1:400; Chemicon, Temecula, CA) and 5% normal goat serum at room temperature (2 hours) and then at 4°C (14–16 hours). After three brief rinses with TBS, the sections were incubated with the secondary antibody (Alexa 594-conjugated red anti-mouse, 1:600, for anti-ChAT; Alexa 488-conjugated green anti-rabbit, 1:600, for anti-CR; Molecular Probes, Eugene, OR) diluted in TBS for 1 hour. After three brief rinses in TBS, sections were mounted out of distilled water on glass slides and coverslipped 30 minutes later with Krystalon 64969 (EM Science Harleco). As control experiments, we omitted either primary antibody from the staining schedule and observed no evidence of cross-reactivity between anti-CR and anti-ChAT with immunofluorescence. Sections were analyzed using a fluorescence microscope (BX-40; Olympus, Tokyo, Japan) equipped with the appropriate filters. Photomicrography was performed with an Optronics microfire digital camera (model 99808; Optronics, Goleta, CA), and digital photographs were edited using Adobe Photoshop 5.0 and Adobe Illustrator 10.0 (Adobe Systems Inc., San Jose, CA).

Quantitative image analysis of double labeling

At each embryonic age, BrdU-CR double-labeled neurons were analyzed at five comparable coronal striatum levels selected at 0.75- ± 0.15-mm intervals, by using the rat atlas of Paxinos and Watson as a guide (1998; see Fig. 1A). The selection included two postcommissural levels caudal to the level of decussation of the anterior commissure (equivalent to sections –2.56 and –1.4 mm with respect to the Bregma; Paxinos and Watson, 1998), a level at which the anterior commissure formed the ventral border of the neostriatum (equivalent to section –0.26 mm; Paxinos and Watson, 1998), and two levels rostral to the decussation of the anterior commissure (equivalent to 1.00 mm and 2.2 mm; Paxinos and Watson, 1998). The dorsal, medial, and lateral limits of the neostriatum were well defined (Paxinos and Watson, 1998). Ventrally, the neostriatum interfaced with the amygdala and substantia innominata in its postcommissural part and with the nucleus accumbens in its precommissural division. We delimited, at the two precommissural levels, the ventral limit of the neostriatum from the nucleus accumbens with a line that extended from above the ventralmost part of the lateral ventricle medially to the tapered external capsule laterally, at an angle of 25° to 30° below the axial plane (see Fig. 1A,B).

Striatal distribution of single-labeled CR-immunoreactive (-IR) neurons and double-labeled BrdU-CR neurons was plotted by using a system for image analysis. The left hemisphere was used for all quantitative analysis. The system consists of a light microscope (BX40; Olympus) equipped with an X-Y movement-sensitive stage (BioPoint XYZ; LEP, Hawthorne, NY), a Z-axis indicator (MT12 microcator; Heidenhain, Traunreut, Germany), and a video camera (DC200; DAGE, Michigan City, IN) coupled to a computer containing software for computer-assisted image analysis (Stereo Investigator; MicroBrightField Inc., Colchester, VT). The software allows drawing of outlines of striatal sections at low (×10 objective) magnification and plotting of positions of single (CR)- or double (BrdU-CR)-labeled neurons evaluated at high (×40 objective) magnification. Photomicrography was performed with an Optronics Microfire digital camera (model 99808; Optronics), and digital photographs were edited using Adobe Photoshop 5.0 and Adobe Illustrator 10.0 (Adobe Systems Inc.).

Three animals from each BrdU-injected age group were selected for analysis. Selection was based on clarity of single- and double-immunohistochemical labeling, least-color mixing of chromogens, low background staining, and optimal tissue preservation. The nickel-enhanced DAB reaction product used as a chromogen for BrdU immunohistochemistry revealed blue-black BrdU-containing nuclei. In contrast, DAB-labeled CR-IR neuronal cell bodies were light brown and often displayed staining of associated dendrites or axons (see Fig. 2A–D). BrdU-IR nuclei of double-labeled cells took the form of a stippled pattern (see Fig. 2B), several large coalescent clumps (see Fig. 2C), or a solid uniform blue-black reaction product (see Fig. 2D). A double-labeled neuron was defined as having at least three speckles of blue-black BrdU nuclear reaction product within the brown CR-IR cytoplasm (see Fig. 2B). Care was taken to exclude instances of false-positive double labeling occurring as a result of BrdU-positive nuclei in close proximity to, but not within, the cytoplasm of CR-IR neurons. A 3% double-labeling index (BrdU-CR double-labeled neurons/total CR-IR neurons) was selected as the limit for "significant" double labeling. A double-labeling index greater than 10% was referred to as "maximal" double labeling (Sadikot and Sasseville, 1997).

Stereology

Unbiased sterelogical estimates of the total number of neostriatum CR-IR neurons were obtained by applying

the optical fractionator (Gundersen et al., 1988; West et al., 1996; Luk and Sadikot, 2001; Luk et al., 2003) with Stereo Investigator. The rostral and caudal limits of the neostriatum were determined (equivalent to Bregma 2.20 to –3.80 mm; Paxinos and Watson, 1998), and every sixth serial section of 50 μm within this volume was examined. Typically, 13 coronal sections at 300 μm intervals were analyzed throughout the reference volume (see Fig. 3A). Mean section thickness after immunohistochemical processing, mounting, and coverslipping was 17 μm (tissue shrinkage effect), as measured with a z-axis microcator. Sampling of the neostriatum was performed by randomly translating a grid with 300- × 300-μm squares onto the section of interest (see Fig. 3B) and applying an optical dissector consisting of an 80- × 80- × 10-μm brick (see Fig. 3C). Each section contained 10–121 sampling sites depending on its surface area. Sections were analyzed by using a ×100 lens (oil, numerical aperture of 1.3, with matching condenser). The optical fractionator was used to determine the total number of neurons. For analysis of morphology, a four-ray isotropic nucleator probe (Gundersen et al., 1988) was also applied to estimate the cross-sectional area and volume of CR-IR interneurons. The most prominent nucleolus was taken as the unique identifier in sections counterstained for Nissl substance. The longest axis of each cell was determined during application of the nucleator, and the cells were divided into six subgroups based on size (see Fig. 3D)

Neurogenesis gradient analysis

To verify lateral-to-medial or a ventral-to-dorsal spatial neurogenesis gradients, two sections of the precommissural neostriatum (equivalent to Bregma 1.00 mm and −0.26 mm; Paxinos and Watson, 1998) were subdivided geometrically into four quadrants (see Fig. 4B). Counts of CR-IR neuron labeling and BrdU-CR double labeling within each of the four quadrants (or lateral and medial halves) were considered collectively at the two striatal levels. To determine dorsal-to-ventral gradients, the dorsal and ventral halves of sections from either the precommissural (equivalent to Bregma 2.20 mm, 1.00 mm) or the postcommissural (Bregma 1.40 mm, –2.56 mm) striatum were analyzed.

The double-labeling index of CR-IR neurons was averaged for 3-day intervals (E13–15, E16–18, E19–21), and comparisons were made among the three resulting groups. Values for the mean double-labeling index in quadrants or halves were plotted (see Fig. 4B,C). A two-way mixed ANOVA procedure and Tukey's HSD post hoc test was used for statistical analysis. Because the data were expressed as a percentage, the ANOVA and Tukey's HSD tests were repeated with Arc Sin-transformed data. All main and interaction effects were calculated with statistical analysis software (SAS 6.12; SAS Institute Inc, Cary, NC; or Datasim 1.1; Drake Bradley, Bates College, ME).

Patch-matrix distribution of CR-IR interneurons

Estimates of CR-IR cell density in the patch, the matrix, and the "intermediate zone" were made for one section (equivalent to Bregma 1.00 mm; Paxinos and Watson, 1998) in eight animals. The "intermediate zones" were defined as annular areas extending 50 μm beyond the patch perimeter (van Vulpen and van der Kooy, 1996). Patch-matrix boundaries were determined by using CB immunostains on adjacent sections. Of note, the dorsolateral part of the neostriatum stains poorly with CB. This region was excluded from patch-matrix analysis. A two-way mixed ANOVA procedure and Tukey's HSD post hoc test were applied to determine statistical differences in neuronal number and density.

Animals injected with BrdU either between E13 and E15 (n = 6, with two animals injected on each embryonic day) or during the E16–18 time interval (n = 6, with two animals injected on each embryonic day) were compared to determine whether the birth date of CR-IR neurons differs with respect to different striatal compartments. A two-way mixed ANOVA procedure and Tukey's HSD post hoc test were applied to determine statistical differences in double-labeling index. When comparing percentages of double-labeled cells, an additional Arc Sin-transformation procedure was applied.

RESULTS

Distribution, morphology, and stereological estimate of total number of neostriatum CR-IR interneurons

CR-IR interneurons were nonhomogeneously distributed in the neostriatum (Fig. 1A,B). The most prominent density gradient was in the rostrocaudal axis, with the highest concentrations of CR-IR neurons in the rostral precommissural neostriatum and the lowest concentrations in the caudal striatum (Fig. 1A). The mean number (±SEM, n = 30) of CR-IR interneurons at distinct rostrocaudal coronal levels (Paxinos and Watson, 1998) was 256 ± 19, 2.20 mm; 209 ± 12, 1.00 mm; 166 ± 10, −0.26 mm; 43 ± 5, –1.40 mm; 21 ± 2, –2.56 mm. The medial aspect of precomissural striatum contained twice as many neurons as the lateral half (Fig. 1A,B). The highest density of CR-IR cells was in the dorsomedial quadrant, with fewer neurons in the dorsolateral and ventromedial quadrants and only a light population density in the ventrolateral quadrant. Our observed rostral-to-caudal (Bennett and Bolam, 1993) and dorsomedial-to-ventrolateral (Figueredo-Cardenas et al., 1996) gradients are in keeping with previous observations.

An estimate of the total number of CR-IR interneurons was determined by unbiased stereology using the optical fractionator method (Gundersen et al., 1988; West et al., 1996; Luk and Sadikot, 2001; Luk et al., 2003). The mean coefficient of error (Gundersen and Jensen, 1987) of CR-IR neuronal counts was 0.11 ± 0.005 (n = 7). The optical fractionator method revealed a total of 13,217 ± 229 (mean ± SEM, n = 7) CR-IR interneurons in the neostriatum contained within a volume of 20.77 ± 0.58 mm^3 (mean ± SEM; n = 7). Based on an estimated 2.54 million (Luk and Sadikot, 2001) to 2.79 million (Oorshot, 1996) neurons in the neostriatum, our analysis indicated that CR-IR interneurons represent approximately 0.5% of all neostriatal neurons in young adult male Sprague-Dawley rats.

The cell bodies of CR-IR interneurons were mainly medium sized and round, oval, or fusiform, and they varied in intensity from light to dark brown on DAB immunostains (Fig. 2). The longest axis of CR-IR cell bodies ranged from 6.2 to 26.5 μm (11.3 ± 0.3 μm; mean ± SEM; Fig. 3D). The

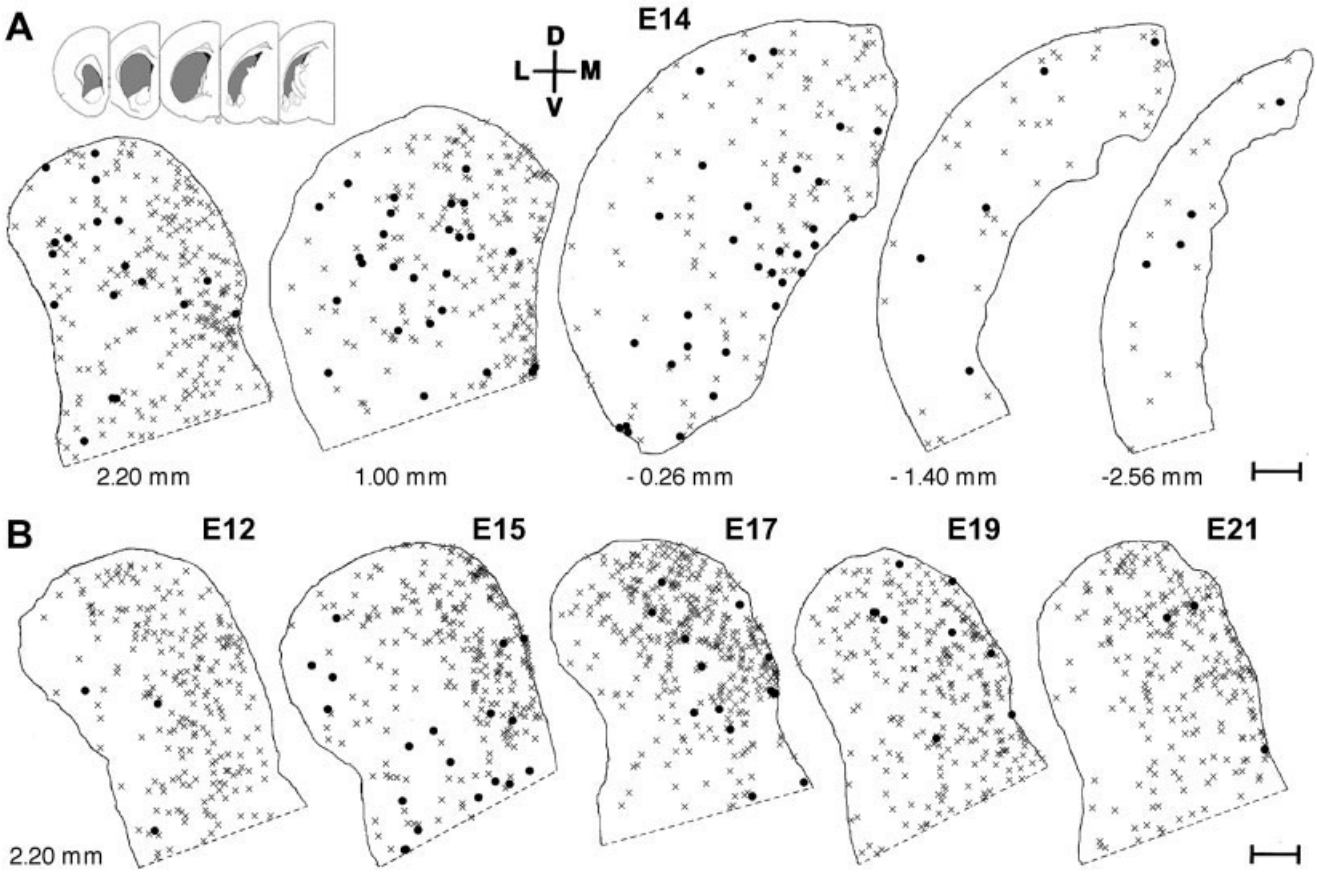

Fig. 1. **A:** Spatial distribution CR-IR interneurons in the neostriatum. Plots containing the location of CR-IR single-labeled (×) and BrdU-CR double-labeled (●) interneurons are shown at five coronal levels through the left striatum (Paxinos and Watson, 1998) in an adult animal exposed to BrdU in utero at E14. Note the rostral-to-caudal and medial-to-lateral density gradients of CR-IR neurons. Orientation and section outlines are also shown (**inset**). **B:** Changes in distribution of double-labeled BrdU-CR neurons during neurogenesis. Location of single-labeled (×) and double-labeled (●) CR-IR interneurons in adult animals exposed to BrdU in utero at different time points of neurogenesis at a single coronal level (equivalent to Bregma 2.20 mm; atlas of Paxinos and Watson, 1998). Note that, early in neurogenesis, BrdU-CR double-labeled cells predominate in the lateral striatum, whereas the latest-born interneurons are located mainly in the dorsomedial quadrant, suggesting a lateral-to-medial gradient of neurogenesis. Scale bars = 500 μm.

mean cross-sectional area of CR-IR cells ranged from 24 to 235 μm^2 (56 ± 3 μm^2; mean ± SEM). The average soma volume ranged from 91 to 3,550 μm^3 (368 ± 23 μm^3; mean ± SEM). Neurons were categorized as small (longest axis ≤7 μm), medium-sized (7.1–20 μm), and large (>20 μm; Chang et al., 1982; Chang and Kitai, 1982; Kawaguchi et al., 1995). Medium-sized cells (7.1–20 μm) made up 91% of all CR-IR neurons, with the majority measuring 7.1–15 μm. Small (7%; Fig. 2C) or large (<2%) neurons constituted a minority population (Fig. 3D). Small cells showed a rostrocaudal gradient of decreasing density similar to that observed for medium-sized cells. These cells were preferentially distributed in dorsomedial zones bordering the periphery of the rostral neostriatum, including the subependymal zones and areas abutting the corpus callosum and external capsule.

Large CR-IR neurons were comparable in size to cholinergic neurons and were distributed nonhomogeneously in the neostriatum. These large neurons were preferentially localized to either the dorsolateral quadrant of the precommissural striatum or the ventral half of the postcommissural striatum close to the boundary with the globus pallidus. Scattered large CR-IR cells were found in the dorsomedial neostriatum close to the corpus callosum or subpendymal area. To determine whether these large cells are also cholinergic, sections were stained by double immunofluorescence using antibodies to ChAT and CR. Although double labeling was noted in other forebrain areas, including the medial septum-diagonal band complex (Fig. 2G,H), there was no instance of double labeling of striatal CR-IR neurons and cholinergic neurons in the neostriatum (Fig. 2E,F). Of note was that the majority of CR-IR and ChAT-IR neurons in the medial septal-diagonal band of Broca complex were not doubly labeled, in keeping with previous studies of this region (Kiss et al., 1997). However, there were a few instances of double-labeling noted in this area. For example, in one section (Bregma 0.7 mm), 107 CR-IR and 185 ChAT-IR neurons were counted in the medial septal-diagonal band complex. We found 13 instances of immunofluorescence double labeling with CR-IR and ChAT-IR in this region. Most of these double-labeled cells contained relatively weak CR-IR immunoflu-

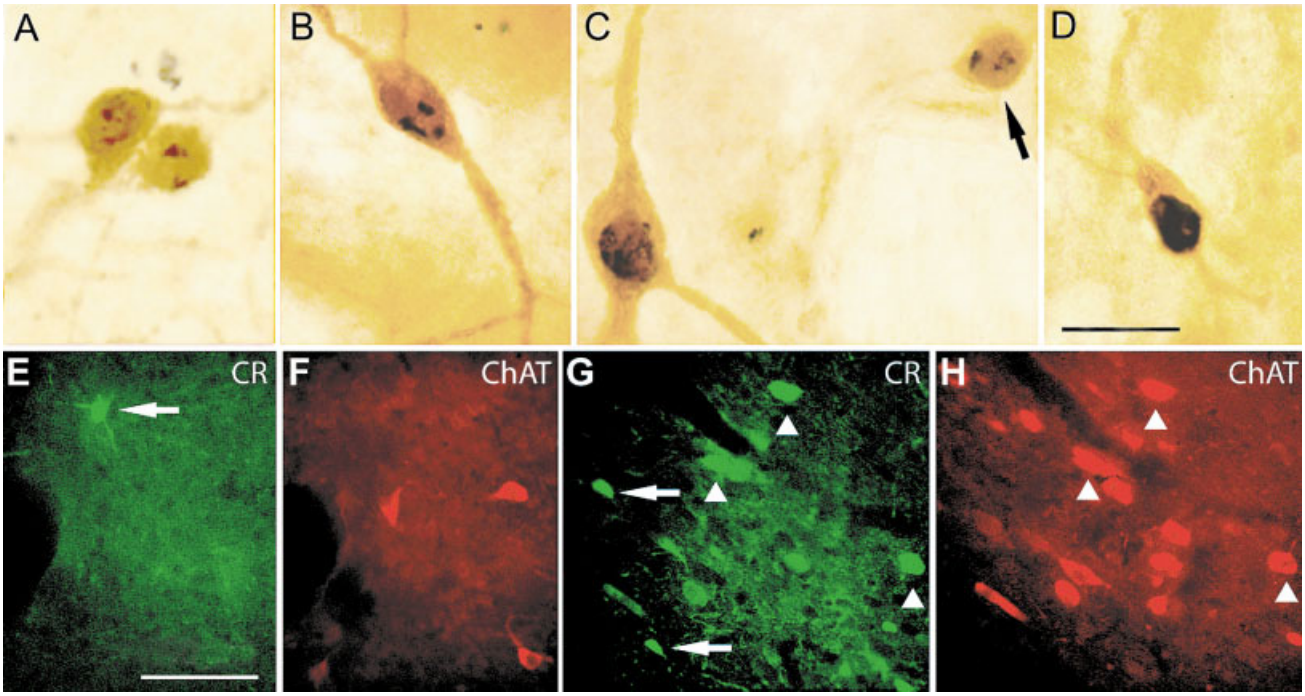

Fig. 2. Photomicrographs of BrdU-CR double-labeled interneurons in the striatum (**A–D**) and examples of analysis to determine possible CR/ChAT colocalization in the basal forebrain (**E–H**). A: Two CR-IR cells, each showing two BrdU-positive stipples. These cells do not meet the criteria used for double labeling, since they contain fewer than three BrdU-positive stipples. B–D: Examples of CR-IR cells counted as doubly labeled, including cells with three BrdU-IR stipples (B), a coalescent pattern of nuclear staining (C), or solid BrdU-IR nuclear staining (D). Note the small CR-BrdU cell (<7 μm diameter) indicated by the arrow (C) alongside a medium-sized double-labeled cell (10–15 μm category). E–H: Colocalization of CR and ChAT in the striatum (E,F) or medial septum-diagonal band area (G,H). No examples of colocalization between CR-IR and ChAT-IR neurons were observed in the neostriatum (E,F), whereas a few large (>20 μm) CR-IR cells colocalized with ChAT-IR in the septum (G,H). Arrows denote single-labeled CR-IR cells, and arrowheads indicate large cells doubly labeled for ChAT-IR and CR-IR. Scale bar = 10 μm in D (applies to A–D); 100 μm in E (applies to E–H).

orescence, except for three cells localized in the horizontal limb of the diagonal band (Fig. 2G,H).

Timetable and spatial gradients of neurogenesis of CR-IR interneurons

The double-labeling index of CR-IR interneurons (BrdU-CR double-labeled cells/total CR-IR cells) in the neostriatum was "maximal" (>10%) between E14 and E17, with a peak at E15 (Fig. 4A). "Significant" double labeling (>3%) occurred between E13 and E19. CR-IR interneurons showed no significant neurogenesis gradient in the rostrocaudal axis (Fig. 5). In contrast, a strong lateral-to-medial gradient neurogenesis gradient was present (Fig. 4B). CR-IR neurons in the lateral half of the striatum became postmitotic at a significantly earlier age than CR-IR neurons occupying the medial half. In the E13–15 group, the double-labeling index was significantly higher in the lateral half compared with the medial half (ANOVA, Tukey's HSD test, $P < 0.0001$). On the other hand, in the E16–18 group, double-labeling index was significantly higher in the medial part of striatum compared with lateral part (ANOVA, Tukey's HSD test, $P < 0.05$). The double-labeling index in the medial half of the striatum in the E19–21 group remained higher than that in the lateral part, but this result was not statistically significant (ANOVA, Tukey's HSD test, $P > 0.05$; Fig. 4B). There was no detectable ventral-to-dorsal gradient of neurogenesis for CR-IR neurons when the entire rostrocaudal extent of the striatum was considered collectively. Finally, there was no statistically significant difference in neurogenesis time course of neurons in dorsal or ventral halves when precommissural or postcommissural levels were analyzed separately. Because data were expressed as a percentage, we validated statistical significance using an Arc Sin transformation and obtained similar results.

To discern further the gradients of neurogenesis in the precommissural striatum, we compared the double-labeling index in separate quadrants (Fig. 4C). The neurogenesis time course of CR-IR neurons was virtually identical in the dorsolateral and ventrolateral quadrants [Tukey's HSD test, $q(144) \leq 0.3$, $P > 0.05$]. These lateral quadrants contain the earliest-born neurons. Neurons in the ventrolateral quadrant were born prior to those in the ventromedial quadrant (Tukey's HSD test, $P < 0.01$). In turn, neurons in the ventromedial quadrant were born prior to those in the dorsomedial quadrant (Tukey's HSD test, $P < 0.05$). When the same test was performed on Arc Sin-transformed data, significance was marginal, suggesting that the gradient between the two medial quadrants was minor. As expected, neurons in the dorsolateral quadrant were born significantly earlier than those in the dorsomedial quadrant (Tukey's HSD test, $P < 0.01$). These data confirm that the strongest neurogenesis gradients are in the lateral-to-medial axis, with only marginal dor-

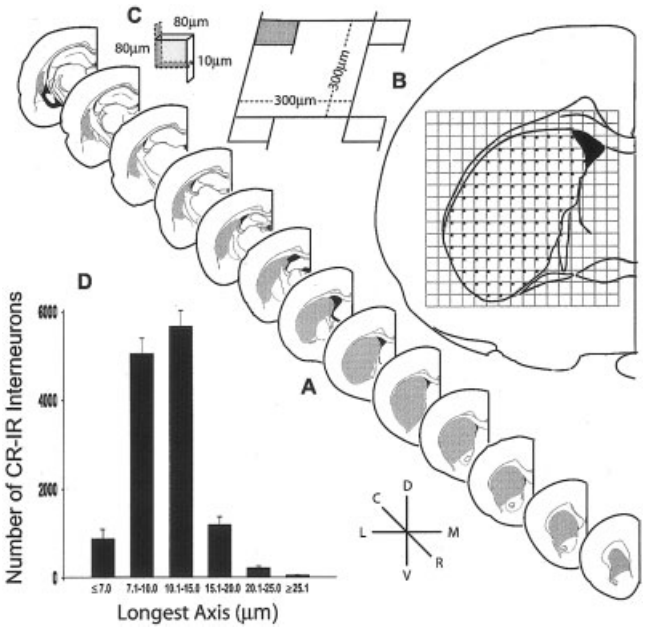

Fig. 3. Sampling scheme used for stereological quantification of neostriatum CR-IR interneurons. **A:** Thirteen coronal sections at regular intervals spanning the entire striatum were selected for stereological analysis (adapted from the atlas of Paxinos and Watson, 1998). **B:** Sampling sites were located at the intersections of a 300- × 300-μm grid placed over the region of interest with the StereoInvestigator software. **C:** 80- × 80-μm counting frames with a depth of 10 μm were applied at each sampling site. Cells in contact with exclusion lines (dotted) and planes (shaded) were not included in the counting procedure. **D:** Histogram showing CR-IR cell size with the longest axis measurement.

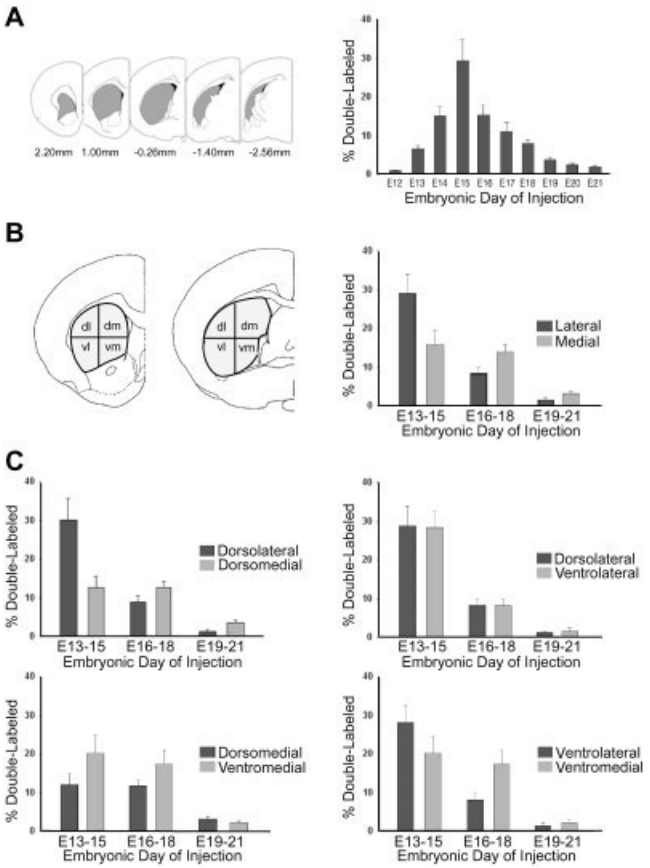

Fig. 4. **A:** Neurogenesis timetable of CR-IR interneurons in the neostriatum. The combined proportion of BrdU-CR double-labeled cells in five representative coronal sections (left) was quantified for animals injected with BrdU on each embryonic day from E12 to E21. Neurogenesis of CR-IR interneurons spans from E13 to E19 (>3% doubly labeled), with maximal neurogenesis (>10% doubly labeled) between E14 and E17 and a peak at E15. **B,C:** Histograms illustrating the BrdU-CR double-labeling index in different halves or quadrants of the precommissural striatum after in utero exposure to BrdU at different embryonic ages. B: Early-born interneurons appear predominantly in the lateral striatum; later-born cells are found mainly in the medial half. C: Analysis of double-labeling index in different quadrants. No significant differences in the proportion of double-labeled cells were observed between lateral quadrants. CR-IR neurons are born first in the lateral quadrants, followed by birth of cells in the ventromedial quadrant and, finally, the dorsomedial quadrant.

soventral differences. In summary, neurons in the lateral quadrants were born earliest, followed in partially overlapping sequence by ventromedial neurons and finally dorsomedial neurons.

Differential neurogenesis with respect to patch-matrix compartments

In approximately 60% of the neostriatum, the intensity of CB immunoreactivity allowed distinction between patch-matrix compartments. The dorsal and lateral territory of the neostriatum was poor in CB immunoreactivity, and patches could not be distinguished in the "sensorimotor" sector based on this marker (Gerfen et al., 1985). CR-IR neurons were localized in both CB-poor patches and CB-rich matrix compartments. We noted a higher density of CR-IR neurons in an "intermediate" or "annular" zone surrounding the patches (Faull et al., 1989, van Vulpen and van der Kooy, 1996), within a 50-μm distance from the CB-IR-defined patch boundary (Fig. 6D,E).

The number and density of CR-IR interneurons was quantified in different striatal compartments (Fig. 6A,B) in the precommissural striatum (equivalent to Bregma 1.00 mm; Paxinos and Watson, 1998). Most CR-IR neurons were in the matrix compartment. Only 3.6% of CR-IR interneurons located in areas with well-demonstrated CB-defined patch-matrix compartments were localized to patches. The mean (±SEM) density of CR-IR cells was significantly different in the patch compartment (17 ± 2) compared with the matrix (27 ± 2; one-way within ANOVA, Tukey's HSD test, $P < 0.05$). The intermediate zone of the matrix had a significantly higher CR-IR cell density (39 ± 5) compared with either patches (17 ± 2; one-way within ANOVA, Tukey's HSD test, $P < 0.01$) or the rest of the matrix (24 ± 2; one-way within ANOVA, Tukey's HSD test, $P < 0.05$).

We determined whether there was a relationship between birth date and localization within a specific compartment of the striatal mosaic. CR-IR neurons in the patch compartment are more likely to become postmitotic during the early time interval (E13–15) compared with the later time period (E16–18; two-way mixed ANOVA, Tukey's HSD test, $P < 0.001$; Fig. 6C). In fact, after E17, no instances of BrdU-CR double labeling were found in

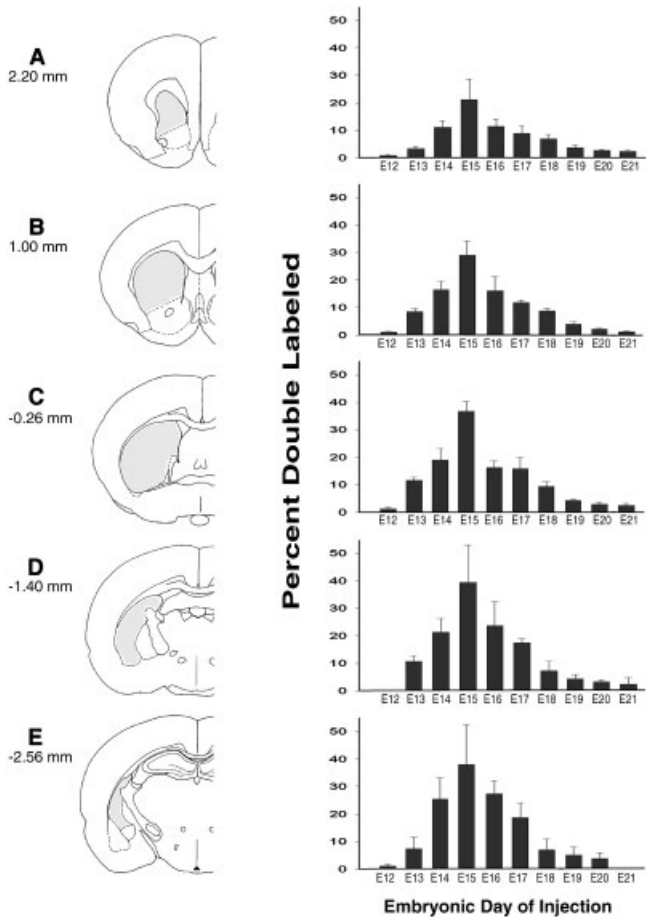

Fig. 5. Histograms illustrating proportion of double-labeled BrdU-CR interneurons in five representative coronal sections of the neostriatum (**A–E**). Collective comparison of the histograms from different coronal levels does not reveal a rostrocaudal neurogenesis gradient.

patches. Double-labeling index in the intermediate zone was not significantly different between the two age intervals. Neurons in the matrix compartment had a greater tendency to be born at E16–18, but the difference was not statistically significant. Finally, the double-labeling index of patch CR-IR interneurons was significantly higher than double-labeling index of matrix CR-IR neurons in the E13–15 group ($P < 0.01$), whereas no significant difference was found in double-labeling index of different compartments in the E16–18 group ($P > 0.05$). The data suggest that CR-IR neurons of the patch compartment are mainly an early-born population, whereas those of the intermediate zone and the rest of the matrix are born during a broader period of neurogenesis.

Patch-matrix compartments were also demonstrated in animals exposed to BrdU at either earlier (E13,14, or 15) or later (E18 or 19) dates. Early injections labeled BrdU-IR-rich patches. Later injections demonstrated a BrdU-IR-rich matrix and BrdU-IR-poor patches. This form of patch or matrix labeling in early- or late-BrdU-injected animals has also been noted in previous studies (van der Kooy and Fishell, 1987; Song and Harlan, 1994; Sadikot and Sasseville, 1997). The BrdU/CR double-immunostained material was used to describe patterns of arborization of appendages of CR-IR cell bodies in either patch or matrix compartments (Fig. 7A–D). This type of analysis requires relatively high spatial resolution and is therefore best performed in the same section. Some neurons in either patch or matrix compartments showed processes that could be followed across boundaries to the complementary mosaic compartment (Fig. 7A–J). Neurons with appendages that crossed boundaries were often located in the intermediate zone, with processes in some cases extending to both the patch and the rest of the matrix compartment (Fig. 7C,D).

DISCUSSION

The main findings of this study are that 1) CR-IR striatal interneurons represent approximately 0.5% of all neostriatum neurons in young adult male Sprague-Dawley rats; 2) CR-IR neurons that populate the neostriatum go through final mitosis between E13 and E19 (>3% doubly labeled), with maximum neurogenesis (>10% doubly labeled) between E14 and E17 and a peak at E15; 3) there is a prominent lateral-to-medial gradient of neurogenesis (rostrocaudal and dorsoventral gradients are weak or not significant); and 4) CR-IR neurons of the patch compartment are born early (E13–15). CR-IR neurons that occupy the matrix compartment become postmitotic over a broader period of neurogenesis.

Distribution, morphology, and total number of CR-IR interneurons in the striatum

The striatum contains mainly medium-sized GABAergic projection neurons and small populations of largely distinct cholinergic neurons and GABAergic interneuron subtypes (Kitai et al., 1979; Bolam et al., 1983, 1984). Distinct subtypes of interneurons containing GABA colocalize the peptide SS (DiFiglia and Aronin, 1982) or the calcium binding proteins PV (Gerfen et al., 1985) or CR (Jacobowitz and Winsky, 1991; Résibois and Rogers, 1992; Bennett and Bolam, 1993; Kubota et al., 1993; Figueredo-Cardenas et al., 1996; Sadikot et al., 1996). Unbiased stereology estimates of total number of neurons in the rodent striatum are derived mainly from work in Sprague-Dawley (S-D) rats (Oorschot, 1996; West et al., 1996; Luk and Sadikot, 2001; Luk et al., 2003), with a few studies in Wistar rats (Larsson et al., 2001) or gerbils (Dam, 1992). Data are available for the total number of neostriatum principal neurons (2.79 million, Oorschot, 1996; 2.54 million, Luk and Sadikot, 2001), SS-positive (21,300, West et al., 1996), NPY-positive cells (14,355, Larsson et al., 2001), PV-positive cells (16,875, Luk and Sadikot, 2001; 16,597, Larsson et al., 2001), and cholinergic interneurons (6,803, Larsson et al., 2001). SS-positive neurons, therefore, make up 0.8% of all neostriatum neurons, whereas PV-IR and cholinergic neurons make up 0.7% and 0.3% of the neuronal population, respectively. The present study suggests that CR-IR neurons account for 0.5% of all neostriatum neurons.

These results indicate that interneurons make up approximately 2.3% of neostriatum neurons, somewhat lower than estimates based on data from nonstereological studies (for reviews see Bolam and Bennett, 1993; Kawaguchi et al., 1995). Despite their small numbers, the synaptic position and chemical anatomy of interneurons

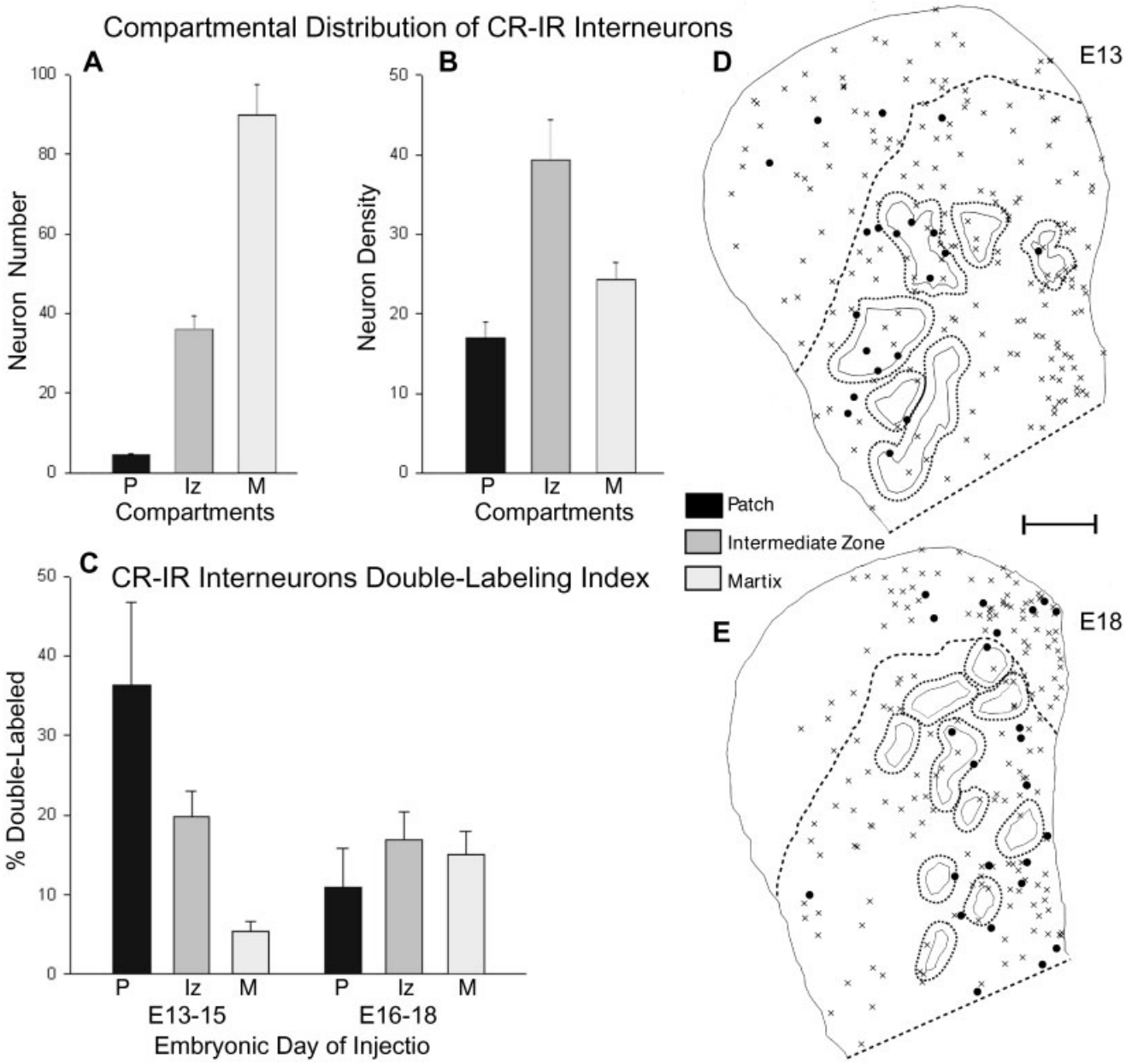

Fig. 6. Compartmental distribution of CR-IR interneurons quantified according to their location within the patch (P), intermediate zone (IZ), or matrix (M) compartments. **A,B:** Results are shown as absolute neuron numbers in A or neuronal densities (neurons/mm^2 ± SEM) in B. CR-IR neurons are located mainly in the matrix, with highest density in the intermediate zone. **C:** Analysis of interneurons in each compartment according to their birth date revealed that most early-born neurons were located in patches, whereas matrix neurons were born over a broader period. **D,E:** Plots of CR single-labeled (×) and BrdU-CR double-labeled (●) interneurons in neostriatum coronal sections (Bregma 1.00 mm) from animals exposed in utero to BrdU at either E13 or E18. The dashed line denotes the boundary between the calbindin-poor dorsolateral zone and the calbindin-rich area, where patch-matrix identification is possible. Limits of patches or the intermediate zones are delineated by solid or dotted lines, respectively. Scale bar = 500 μm.

likely allow powerful modulation of the physiology of the neostriatum (cf. Lapper et al., 1992; Kita, 1993; Rudkin and Sadikot, 1999; Sidibé and Smith, 1999; Koos and Tepper, 1999; Ramanathan et al., 2002). It is interesting that the relative ratio of interneurons may differ in rodents compared with primate species. Whereas PV-IR (Luk and Sadikot, 2001) and SS-IR (West et al., 1996) neostriatal interneurons outnumber CR-IR interneurons (present study) in S-D rats, in humans and squirrel monkeys neostriatal CR-IR interneurons outnumber PV-IR and SS-IR interneurons by a ratio of approximately 3:1 (Wu and Parent, 2000). This finding possibly suggests increased functional importance of CR-IR neurons in primates compared with other interneuron subtypes.

CR-IR interneurons are distributed throughout the neostriatum. There is a strong cell density gradient along

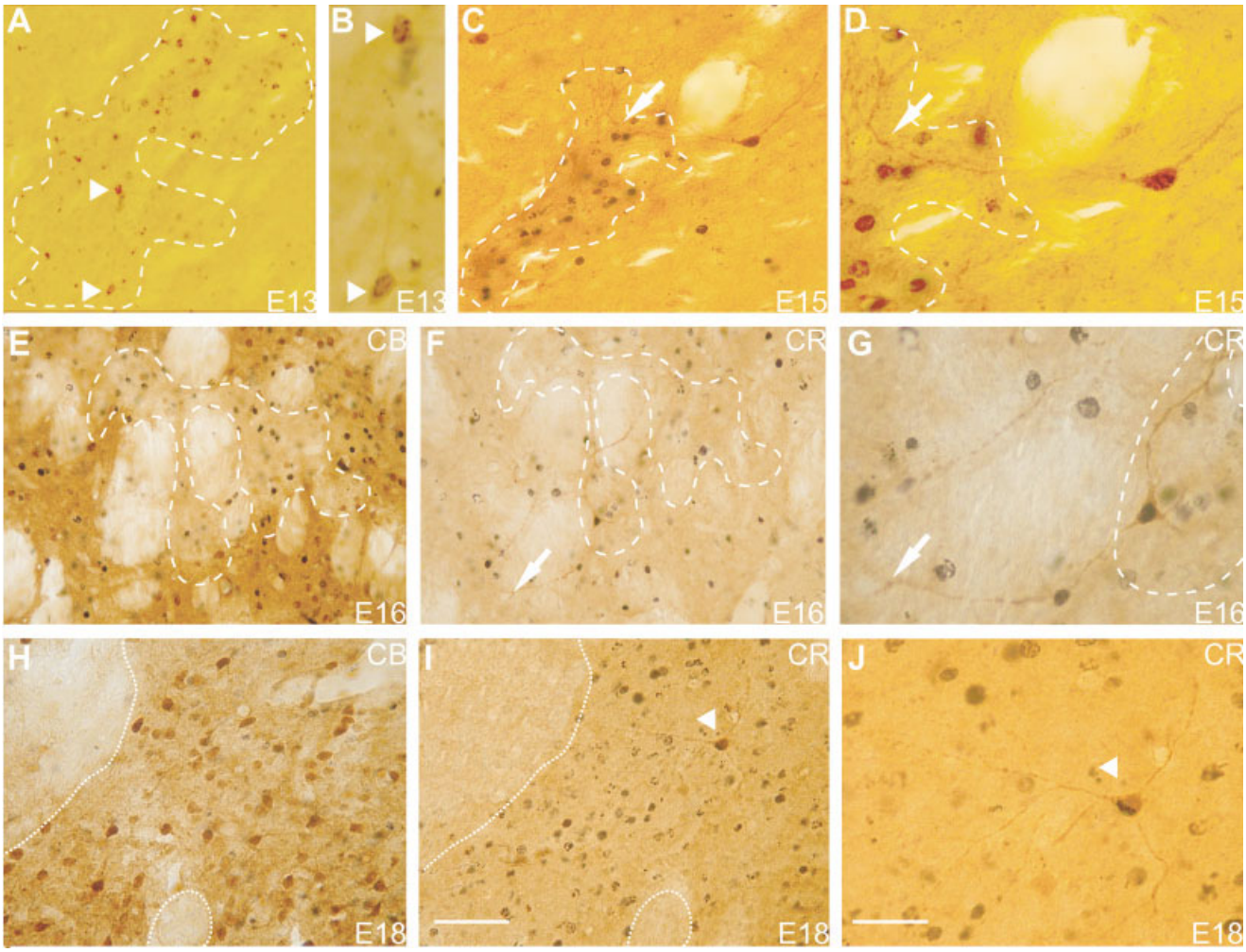

Fig. 7. Photomicrographs of adjacent BrdU-CR and BrdU-CB double-immunolabeled sections used for descriptive analysis of morphological distribution of CR-IR neurons with respect to patch-matrix compartments. In animals exposed to BrdU at early intervals (E13–15), the boundaries of patches were delineated by BrdU immunostaining. **A,B:** CR-IR neurons (arrowheads) are noted in a BrdU-rich patch in an animal exposed to BrdU at E13 (dashed line). **C,D:** A BrdU-rich patch in an animal exposed to BrdU at E15 contains a process (arrow) of a BrdU-CR double-labeled neuron located in the intermediate zone of the matrix. **E–G:** Adjacent sections stained for BrdU-CB (E) or BrdU-CR (F,G) in an animal exposed to BrdU at E16. The dashed line in E–G denotes the boundaries of a patch identified on the basis of CB-poor (E) immunostaining. E and F were taken at similar magnification, and G is a high-power view. A BrdU-CR double-labeled interneuron in a patch (F,G) sends a process (arrow) into the matrix. **H–J:** Adjacent sections stained for BrdU-CB (H) or BrdU-CR (I,J) in an animal exposed to BrdU at E18. The dotted lines in H–J denote boundaries of the pencil fibers of the striatum, which are identified as a morphological reference. The CB-rich matrix compartment is shown in H. The adjacent BrdU-CR-immunostained section at identical magnification (I) and at higher magnification (J) shows a double-labeled interneuron with processes restricted to the matrix compartment. Scale bar = 50 μm in I (applies to A,C,E,F,H,I); 25 μm in J (applies to B,D,G,J).

the rostrocaudal axis of the neostriatum, in keeping with previous observations (Bennett and Bolam, 1993). A moderate mediolateral density gradient is also observed in the precommissural neostriatum. The highest density of CR-IR interneurons is seen in the dorsomedial quadrant of the precommissural striatum, with an intermediate density in the ventromedial quadrant and the lowest density in lateral quadrants, largely in keeping with previous work (Figueredo-Cardenas et al., 1996). A dorsolateral band of striatal tissue, corresponding to an area that labels poorly for CB, contains only scattered CR-IR neurons.

The distribution of CR-IR neurons contrasts sharply with that of another prominent population of GABAergic interneurons that expresses the calcium binding protein PV. PV-IR density is higher in the lateral part of the precommissural striatum compared with the medial parts (Gerfen et al., 1985; Celio, 1990; Cowan et al., 1990; Kita et al., 1990; Kubota and Kawaguchi, 1993; Kubota et al., 1993; Bennett and Bolam, 1994; Sadikot et al., 1996; Figueredo-Cardenas et al., 1996; Sadikot and Sasseville, 1997). Comparison of maps of CR-IR (present study) and PV-IR neurons (Sadikot and Sasseville, 1997) shows that the distribution gradients in the neostriatum are largely complementary. Whereas PV-IR neurons are located preferentially in "sensorimotor territories" of the rodent neostriatum, CR-IR neurons distribute preferentially in neo-

striatum areas that receive afferents mainly from allocortical-mesocortical areas (Webster, 1961; McGeorge and Faull, 1989; for review see Berendse et al., 1992). In primates, these complementary areas correspond broadly to either the precommissural putamen (sensorimotor territory) or the caudate and rostral putamen (associative territory), respectively (Kemp and Powell, 1970; Kunzle, 1975; Goldman and Nauta, 1977; Yeterian and Van Hoesen, 1978; Smith and Parent, 1986; for review see Sadikot et al., 1992a,b).

Consistent with previous studies (Bennett and Bolam, 1993), CR-IR interneurons are mainly oval or round and less frequently fusiform. Most cell bodies (91%) are medium-sized (7–20 μm, longest axis), and most have cell diameters between 7.1 and 15 μm (82%). In comparison with other medium-sized interneurons, CR-IR neurons tend to have smaller soma (SS-IR, 10–35 μm; PV-IR, 15–35 μm; Kubota et al., 1993; Kawaguchi et al., 1995; Figueredo-Cardenas et al., 1996). A few small neurons, ≤7 μm, and rare large neurons, >20 μm, were also identified. Small or large cells may represent a separate subpopulation or may be part of a continuous distribution of CR-IR neurons. Some of these small CR-IR cells may belong to the neuroglioform group identified in previous Golgi impregnation studies (Chang et al., 1982). In the human striatum, most large CR-IR interneurons colocalize with cholinergic markers (Cicchetti et al., 1998). In contrast, in the present study, we demonstrate that large CR-IR neurons do not colocalize with cholinergic markers in the rodent neostriatum, in keeping with previous publications (Bennett and Bolam, 1993; Figueredo-Cardenas et al., 1996). In some studies, a small proportion of CR-IR neurons colocalizes with PV-IR (Kubota et al., 1993; Figueredo-Cardenas et al., 1996) or SS-IR (Kubota et al., 1993) neurons, whereas other studies did not reveal any significant colocalization of CR-IR neurons with either PV-IR (Bennett and Bolam, 1993) or SS-IR subtypes (Bennett and Bolam, 1993; Figueredo-Cardenas et al., 1996). Rodent CR-IR neurons are therefore a mainly distinct population compared with other striatal neurons.

Neurogenesis of CR-IR interneurons compared with other neurons of the neostriatum

Striatal projection neurons become postmitotic over a broad time interval, between E12 and E22–P2 (E0 corresponds to day of fertilization), with maximal mitosis at E14–18 (Fentress et al., 1981; Bayer, 1984; Marchand and Lajoie, 1986). Interneurons have more restricted timetables of neurogenesis. Striatum cholinergic interneurons are the earliest born, with the majority of neurogenesis occurring between E12 and E15 (Bayer 1984; Marchand and Lajoie, 1986; Semba et al., 1988; Phelps et al., 1989). SS-IR interneurons are born later, during a narrow timetable mainly between E15 and E16 (Semba et al., 1988). PV-IR (Sadikot and Sasseville, 1997) and CR-IR GABAergic interneuron subtypes in the neostriatum have similar timetables of neurogenesis. Both neuronal subtypes show significant neurogenesis between E13 and E20, with maximal neurogenesis between E14 and E17. Whereas CR-IR neurogenesis shows a sharp peak at E15, PV-IR neurogenesis shows a broader peak at E14–17.

Significant differences exist in neurogenesis gradients of striatal subtypes. Projection neurons show a strong ventrolateral-to-dorsomedial gradient (Fentress et al., 1981). In the precommissural neostriatum, prominent "outside-in" (lateral to medial) and caudal-to-rostral neurogenesis gradients are observed (Smart and Sturrock, 1979; Fentress et al., 1981; Bayer 1984; Marchand and Lajoie, 1986). Exceptionally, in the postcommissural striatum, an "inside-out" and rostral-to-caudal gradient was observed in one study (Bayer, 1984). In other studies, caudal-to-rostral and "outside-in" gradients are noted throughout the neostriatum (Smart and Sturrock, 1979; Fentress et al., 1981; Marchand and Lajoie, 1986). Neostriatal cholinergic interneurons show strong caudal-to-rostral neurogenesis gradients (Marchand and Lajoie, 1986; Semba et al., 1988; Phelps et al., 1989) and subtle lateral-to-medial gradients in the precommissural striatum (Semba et al., 1988). PV-IR interneurons show a similar caudal-to-rostral gradient through the neostriatum and outside-in gradients in the precommissural striatum (Sadikot and Sasseville, 1997). SS-IR interneurons do not show significant spatial gradients of neurogenesis (Semba et al., 1988), possibly reflecting a heterogeneous cell population (Rushlow et al., 1996; Sadikot and Sasseville, 1997).

CR-IR interneurons show a prominent lateral-to-medial gradient, as is the case for projection neurons and PV-IR interneurons and, to a lesser extent, cholinergic interneurons. In contrast to cholinergic and PV-IR interneurons, CR-IR neurons show only a weak or absent caudal-to-rostral gradient. The absence of a detectable caudal-to-rostral gradient in our material may reflect the sharp neurogenesis peak seen at E15, possibly masking a gradient occurring over a short interval. In the precommissural striatum, the ventrolateral and dorsolateral quadrants contain the earliest-born CR-IR neurons, followed by the ventromedial quadrant. The latest-born neurons occupy the dorsomedial quadrant. Interestingly, projection neurons show remarkably similar ventrolateral-to-dorsomedial gradients.

The "outside-in" pattern of neurogenesis observed with most neostriatum neuronal subtypes is also seen in other regions of the basal forebrain (Creps, 1974; ten Donkelaar and Dederen, 1979; Bayer and Altman, 1987), suggesting a general organizing principle of neurogenesis of both projection neurons and interneurons in the basal telencephalon (Fentress et al., 1981; Bayer and Altman, 1987; Sadikot and Sasseville, 1997). This contrasts with neurogenesis of projection neurons in the cerebral cortex, where later-born cells migrate past early-born neurons, yielding an "inside-out" pattern (Angevine and Sidman, 1961; Berry and Rogers, 1965; Rakic, 1971). Recent studies suggest that GABAergic interneurons that populate the cortex originate from the ventral telencephalon (de Carlos et al., 1996; Anderson et al., 1997, 2001; Tamamaki et al., 1997; Lavdas et al., 1999; Wichterle, 1999). It would therefore be of interest to determine whether PV-IR and CR-IR subtypes of cortical GABAergic interneurons show timetables and neurogenesis gradients similar to those of their counterparts in the ventral telencephalon. Our preliminary work suggests that cortical and striatal CR-IR interneurons show neurogenesis patterns similar to those of their subcortical counterparts (Sadikot and Rymar, 2000; Rymar and Sadikot, 2001).

Localization and birth date of CR-IR interneurons with respect to patch and matrix compartments

Striatal neurons are disposed to patch and matrix compartments that may be distinguished on the basis of chemical anatomy or with respect to organization of afferents and efferents (for reviews see Tennyson et al., 1972; Graybiel and Ragsdale, 1978; Herkenham and Pert, 1981; Gerfen, 1992; Sadikot et al 1992b). Cholinergic (Graybiel et al., 1986; van Vulpen and van der Kooy, 1996), SS-IR (Gerfen, 1984; Rushlow et al., 1996), and PV-IR (Cowan et al., 1990) interneurons populate both the patch and the matrix compartments of the striatum. Our results suggest that CR-IR interneurons of the neostriatum are nonhomogeneously distributed with respect to patch-matrix compartments. Calbindin labels the matrix compartment in most striatal areas, except at a dorsolateral band corresponding to an area that receives sensorimotor afferents. This sensorimotor zone is also relatively poor in CR-IR neurons. The calbindin-rich matrix compartment has a significantly higher density of CR-IR neurons compared with CB-poor patches. This difference can be partially attributed to a high concentration of CR-IR interneurons in the peripatch matrix compartment or intermediate zone.

Neurons in either patch or matrix compartments (especially in the intermediate zone) show processes that can be followed across boundaries to the complementary mosaic compartment. This distribution supports the hypothesis that striatal CR-IR interneurons participate in intercompartmental communication. Other interneuron subtypes, including SS-IR (Gerfen, 1984; Rushlow et al., 1996), cholinergic (Bolam et al., 1988; Kubota and Kawaguchi, 1993), and PV-IR (Cowan et al., 1990) neurons also send processes to the complementary mosaic area and may also serve to allow communication between compartments. The peripatch intermediate zone also contains a higher concentration of cholinergic interneurons (van Vulpen and van der Kooy, 1996). Although processes of most projection neurons of the striatum respect compartmental boundaries, a few neurons at the peripatch boundary zone send processes into the patch compartment and may, therefore, serve as an additional substrate for patch-matrix communication (Bolam et al., 1988; Penny et al., 1988).

In the rat, neurons of the patch compartment are generated mainly between E12 and E16, whereas the majority of neurons that occupy the matrix compartment are born between E17 and E20 (Marchand and Lajoie, 1986; van der Kooy and Fishell, 1987; Fishell and van der Kooy, 1991). CR-IR interneurons in the patch comparment are born early, whereas neurons in the peripatch compartment and the rest of the matrix are born over a broader timetable. Striatal cholinergic neurons that populate the patch compartment are also born earlier than their counterparts in the peripatch intermediate zone and in the rest of the matrix (van Vulpen and van der Kooy, 1996, 1998). This finding indicates that compartmental difference in birth date may be a general property of interneurons, analogous to differences in birth dates for projection neurons that occupy the patch or matrix. Such differences in birth date may be due to possible decreased neuronal adhesiveness as neurogenesis progresses, resulting in wider dispersion of later-born neurons (Krushel et al., 1995; van Vulpen and van der Kooy, 1998). Recent work suggests a role for diffusible molecules, including Slit-1 and Netrin-1, in repelling cells from the ventricular zone of the striatal ganglionic eminence zone (Zhu et al., 1999; Hamasaki et al., 2001). Netrin-1 expressed in the ventricular zone may guide later-born matrix neurons into the striatal primordium (Hamasaki et al., 2001). In addition, transcription factors of the homedomain and basic helix-loop-helix (bHLH) gene families may play a role in determining the patch or matrix location of early- or later-born neurons. For example, Dlx1/2 and Ebf1 mutants fail to generate later-born striatal neurons (Anderson et al., 1997; Garel et al., 1999), whereas Mash1 mutants and GSH1,2 double mutants show impaired generation of early-born striatal neurons (Casarosa et al., 1999; Toresson and Campbell, 2001). The available data based on transciption factor mutants do not as yet elucidate mechanisms that may guide the mainly early-born GABAergic interneuron subpopulation to either the patch or the matrix compartment. Further attention to transcription factors, adhesions molecules, or receptors specifically expressed by interneurons may help to elucidate mechanisms by which these subgroups populate different compartments.

Origin of the striatal interneurons

The proliferative neuroepithelium of the lateral ganglionic eminence is the main source of striatal principal neurons (Pakzaban et al., 1993; Deacon et al., 1994; Olsson et al., 1995; Campbell et al., 1995). Recent evidence suggests that most interneurons of the forebrain, including the striatum, arise from the medial ganglionic eminence and neighboring preoptic and anterior entopeduncular area (Olsson et al., 1998; Lavdas et al., 1999; Wichterle et al., 1999; Marin et al., 2000). Studies examining mutants lacking specific transcription factors (e.g., Mash1, NKX2.1) suggest that cholinergic, CR-IR, and SS-IR interneurons that populate both the striatum and the cerebral cortex originate mainly in the medial ganglionic eminence (Sussel et al., 1999; Marin et al., 2000). In the case of CR-IR interneurons, the cell loss in Mash1–/– and NKX2.1–/– mutants is mainly at caudal levels, with less prominent reduction at rostral striatal levels (Marin et al., 2000). Our quantitative study suggests that only 15% of CR-IR interneurons are located caudally to the anterior commissure. This finding leaves open the possibility that some CR-IR interneurons may arise from a source other than the medial ganglionic eminence.

Because PV expression is minimal in the neonatal forebrain, it is not possible to reach a conclusion on the origin of neurons based on study of the available transcription factor mutants, which generally die shortly after birth. The protein product of the NKX2.1 gene is expressed at an early developmental phase, mainly in the medial ganglionic eminence, and is present in most striatal interneurons in adults, including PV-IR cells (Marin et al., 2000). Furthermore, the time course of neurogenesis for striatal PV-IR and CR-IR interneurons is remarkably similar (Sadikot and Sasseville, 1997; present results). Taken together, these findings support the hypothesis that a significant proportion of PV-IR interneurons is also generated from the medial ganglionic eminence. The present evidence does not, however, preclude the possibility that some PV-IR interneurons are generated in the lateral ganglionic eminence. Our recent work on the neurogenesis

period of cortical CR-IR and PV-IR interneurons suggests a period of neurogenesis similar to that of their striatal counterparts (Rymar and Sadikot, 2001), in keeping with the notion that most forebrain interneurons originate in the ventral telencephalon.

A common origin for interneurons of the forebrain in the basal telencephalon has important potential implications for developmental disorders. Events influencing GABAergic or cholinergic neurogenesis at E14–18 (equivalent to gestational age 7–12 weeks in humans; Bayer et al., 1993) would influence the excitability of the entire forebrain and, therefore, potentially contribute to the pathogenesis of a wide variety of developmental disorders, including the cerebral palsies and the epilepsies. We have recently demonstrated that proliferation of GABAergic projection neurons and interneurons originating in the basal telencephalon is dependent on N-methyl-D-aspartate (NMDA) receptor activation (Sadikot et al., 1998; Luk et al., 2003). A wide variety of prenatal insults is mediated by NMDA receptors, including ischemia and toxic exposure to drugs of abuse (e.g., phencyclidine, ethanol; Tabakoff et al., 1991; Deutsch et al., 1998), sedatives, anticonvulsants, and anesthetics (Reich and Silvay, 1989; Jevtovic-Todorovic et al., 1998; Morrell, 1999). Brain injury as early as the first trimester of pregnancy may therefore alter GABAergic cell number and modulate the excitability of the forebrain.

CONCLUSIONS

Striatal neuronal subtypes show distinct patterns of neurogenesis with common features. Cholinergic interneurons are born first, followed by GABAergic interneuron subtypes. Both interneurons and projection neurons occupying the patch compartment are born early in comparison with projection neurons of the matrix. Interneurons occupying the patch compartment are born earlier than most interneurons of the matrix. With the exception of SS-IR subtypes, all striatal interneurons show caudal-to-rostral and lateral-to-medial gradients of neurogenesis. Increasing evidence suggests that GABAergic interneurons of the entire forebrain originate in the ventral telencephalon. Neurogenesis characteristics of specific striatal interneuron subpopulations may, therefore, also be relevant to patterns of neurogenesis of homologous neurons occupying the rest of the forebrain.

ACKNOWLEDGMENTS

The authors thank Marie-Claude Bélanger and Rubina Rangwala for technical and administrative assistance.

LITERATURE CITED

Anderson SA, Eisenstat DD, Shi L, Rubenstein JL. 1997. Interneuron migration from basal forebrain to neocortex: dependence on Dlx genes. Science 278:474–476.

Anderson SA, Marin O, Horn C, Jennings K, Rubenstein JL. 2001. Distinct cortical migrations from the medial and lateral ganglionic eminences. Development 128:353–363.

Angevine JB Jr, Sidman RL.1961. Autoradiographic study of cell migration during histigenesis of cerebral cortex in the mouse. Nature 192:766–768.

Bayer SA. 1984. Neurogenesis in the rat neostriatum. Int J Dev Neurosci 2:163–175.

Bayer SA, Altman J. 1987. Directions in neurogenetic gradients and patterns of anatomical connections in the telencephalon. Prog Neurobiol 29:57–106.

Bayer SA, Altman J, Russo RJ, Zhang X. 1993. Timetables of neurogenesis in the human brain based on experimentally determined patterns in the rat. Neurotoxicology 14:83–144.

Bennett BD, Bolam JP. 1993. Characterization of calretinin-immunoreactive structures in the striatum of the rat. Brain Res 609:137–148.

Bennett BD, Bolam JP. 1994. Synaptic input and output of parvalbumin-immunoreactive neurons in the neostriatum of the rat. Neuroscience 62:707–719.

Berendse HW, Galis-de Graaf Y, Groenewegen HJ. 1992. Topographical organization and relationship with ventral striatal compartments of prefrontal corticostriatal projections in the rat. J Comp Neurol 316: 314–347.

Berry M, Roger AW. 1965. The migration of neuroblasts in the developing cerebral cortex. J Anat 99:691–709.

Bolam JP, Bennett BD. 1993. Microcircuitry of the neostriatum. In: Marjorie A, Ariano MA, Surmeier DJ, editors. Molecular and cellular mechanisms of neostriatal function. Heidelberg: Springer. p 1–19.

Bolam JP, Clarke DJ, Smith AD, Somogyi P. 1983. A type of aspiny neuron in the rat neostriatum accumulates [^{3}H]gamma-aminobutyric acid: combination of Golgi-staining, autoradiography, and electron microscopy. J Comp Neurol 213:121–134.

Bolam JP, Ingham CA, Smith AD. 1984. The section-Golgi-impregnation procedure—3. Combination of Golgi-impregnation with enzyme histochemistry and electron microscopy to characterize acetylcholinesterase-containing neurons in the rat neostriatum. Neuroscience 12:687–709.

Bolam JP, Izzo PN, Graybiel AM. 1988. Cellular substrate of the histochemically defined striosome/matrix system of the caudate nucleus: a combined Golgi and immunocytochemical study in cat and ferret. Neuroscience 24:853–875.

Butcher LL, Hodge GK. 1976. Postnatal development of acetylcholinesterase in the caudate-putamen nucleus and substantia nigra of rats. Brain Res 106:223–240.

Campbell K, Olsson M, Bjorklund A. 1995. Regional incorporation and site-specific differentiation of striatal precursors transplanted to the embryonic forebrain ventricle. Neuron 15:1259–1273.

Casarosa S, Fode C, Guillemot F. 1999. Mash1 regulates neurogenesis in the ventral telencephalon. Development 126:525–534.

Celio MR. 1990. Calbindin D-28k and parvalbumin in the rat nervous system. Neuroscience 35:375–475.

Chang HT, Kitai ST. 1982. Large neostriatal neurons in the rat: an electron microscopic study of gold-toned Golgi-stained cells. Brain Res Bull 8:631–643.

Chang HT, Wilson CJ, Kitai ST. 1982. A Golgi study of rat neostriatal neurons: light microscopic analysis. J Comp Neurol 208:107–126.

Cicchetti F, Beach TG, Parent A. 1998. Chemical phenotype of calretinin interneurons in the human striatum. Synapse 30:284–297.

Cowan RL, Wilson CJ, Emson PC, Heizmann CW. 1990. Parvalbumin-containing GABAergic interneurons in the rat neostriatum. J Comp Neurol 302:197–205.

Creps ES. 1974. Time of neuron origin in preoptic and septal areas of the mouse: an autoradiographic study. J Comp Neurol 157:161–244.

Dam AM. 1992. Estimation of the total number of neurons in different brain areas in the Mongolian gerbil: a model of experimental ischemia. Acta Neurol Scand Suppl 137:34–36.

Deacon TW, Pakzaban P, Isacson O. 1994. The lateral ganglionic eminence is the origin of cells committed to striatal phenotypes: neural transplantation and developmental evidence. Brain Res 668:211–219.

de Carlos JA, Lopez-Mascaraque L, Valverde F. 1996. Dynamics of cell migration from the lateral ganglionic eminence in the rat. J Neurosci 16:6146–6156.

del Rio JA, Soriano E. 1989. Immunocytochemical detection of 5′-bromodeoxyuridine incorporation in the central nervous system of the mouse. Brain Res Dev Brain Res 49:311–317.

Deutsch SI, Mastropaolo J, Rosse RB. 1998. Neurodevelopmental consequences of early exposure to phencyclidine and related drugs. Clin Neuropharmacol 21:320–332.

DiFiglia M, Aronin N. 1982. Ultrastructural features of immunoreactive somatostatin neurons in the rat caudate nucleus. J Neurosci 2:1267–1274.

Faull RL, Dragunow M, Villiger JW. 1989. The distribution of neurotensin receptors and acetylcholinesterase in the human caudate nucleus: ev-

idence for the existence of a third neurochemical compartment. Brain Res 488:381–386.

Fentress JC, Stanfield BB, Cowan WM. 1981. Observation on the development of the striatum in mice and rats. Anat Embryol 163:275–298.

Figueredo-Cardenas G, Medina L, Reiner A. 1996. Calretinin is largely localized to a unique population of striatal interneurons in rats. Brain Res 709:145–150.

Fishell G, van der Kooy D. 1991. Pattern formation in the striatum: neurons with early projections to the substantia nigra survive the cell death period. J Comp Neurol 312:33–42.

Garel S, Marin F, Grosschedl R, Charnay P. 1999. Ebf1 controls early cell differentiation in the embryonic striatum. Development 126:5285–5294.

Gerfen CR. 1984. The neostriatal mosaic: compartmentalization of corticostriatal input and striatonigral output systems. Nature 311:461–464.

Gerfen CR. 1992. The neostriatal mosaic: multiple levels of compartmental organization. Trends Neurosci 15:133–139.

Gerfen CR, Baimbridge KG, Miller JJ. 1985. The neostriatal mosaic: compartmental distribution of calcium-binding protein and parvalbumin in the basal ganglia of the rat and monkey. Proc Natl Acad Sci U S A 82:8780–8784.

Goldman PS, Nauta WJ. 1977. Columnar distribution of cortico-cortical fibers in the frontal association, limbic, and motor cortex of the developing rhesus monkey. Brain Res 122:393–413.

Graybiel AM, Ragsdale CW Jr. 1978. Histochemically distinct compartments in the striatum of human, monkeys, and cat demonstrated by acetylthiocholinesterase staining. Proc Natl Acad Sci U S A 75:5723–5726.

Graybiel AM, Baughman RW, Eckenstein F. 1986. Cholinergic neuropil of the striatum observes striosomal boundaries. Nature 323:625–627.

Grofova I. 1975. The identification of striatal and pallidal neurons projecting to substantia nigra. An experimental study by means of retrograde axonal transport of horseradish peroxidase. Brain Res 91:286–291.

Gundersen HJ, Jensen EB. 1987. The efficiency of systematic sampling in stereology and its prediction. J Microsc 147:229–263.

Gundersen HJ, Bagger P, Bendtsen TF, Evans SM, Korbo L, Marcussen N, Moller A, Nielsen K, Nyengaard JR, Pakkenberg B, et al. 1988. The new stereological tools: disector, fractionator, nucleator and point sampled intercepts and their use in pathological research and diagnosis. APMIS 96:857–881.

Hamasaki T, Goto S, Nishikawa S, Ushio Y. 2001. A role of netrin-1 in the formation of the subcortical structure striatum: repulsive action on the migration of late-born striatal neurons. J Neurosci 21:4272–4280.

Herkenham M, Pert CB. 1981. Mosaic distribution of opiate receptors, parafascicular projections and acetylcholinesterase in rat striatum. Nature 291:415–418.

Jacobowitz DM, Winsky L. 1991. Immunocytochemical localization of calretinin in the forebrain of the rat. J Comp Neurol 304:198–218.

Jevtovic-Todorovic V, Todorovic SM, Mennerick S, Powell S, Dikranian K, Benshoff N, Zorumski CF, Olney JW. 1998. Nitrous oxide (laughing gas) is an NMDA antagonist, neuroprotectant and neurotoxin. Nat Med 4:460–463.

Kawaguchi Y. 1997. Neostriatal cell subtypes and their functional roles. Neurosci Res 27:1–8.

Kawaguchi Y, Wilson CJ, Augood SJ, Emson PC. 1995. Striatal interneurones: chemical, physiological and morphological characterization. Trends Neurosci 18:527–535.

Kemp JM, Powell TP. 1970. The cortico-striate projection in the monkey. Brain 93:525–546.

Kemp JM, Powell TP. 1971. The structure of the caudate nucleus of the cat: light and electron microscopy. Philos Trans R Soc Lond B Biol Sci 262:383–401.

Kiss J, Magloczky Z, Somogyi J, Freund TF. 1997. Distribution of calretinin-containing neurons relative to other neurochemically identified cell types in the medial septum of the rat. Neuroscience 78:399–410.

Kita H. 1993. GABAergic circuits of the striatum. Prog Brain Res 99:51–72.

Kita H, Kosaka T, Heizmann CW. 1990. Parvalbumin-immunoreactive neurons in the rat neostriatum: a light and electron microscopic study. Brain Res 536:1–15.

Kitai ST, Preston RJ, Bishop GA, Koscis JD. 1979. Striatal projection neurons: morphological and electrophysiological studies. Adv Neurol 24:45–51.

Koos T, Tepper JM. 1999. Inhibitory control of neostriatal projection neurons by GABAergic interneurons. Nat Neurosci 2:467–472.

Krushel LA, Fishell G, van der Kooy D. 1995. Pattern formation in the mammalian forebrain: striatal patch and matrix neurons intermix prior to compartment formation. Eur J Neurosci 7:1210–1219.

Kubota Y, Kawaguchi Y. 1993. Spatial distributions of chemically identified intrinsic neurons in relation to patch and matrix compartments of rat neostriatum. J Comp Neurol 332:499–513.

Kubota Y, Mikawa S, Kawaguchi Y. 1993. Neostriatal GABAergic interneurones contain NOS, calretinin or parvalbumin. Neuroreport 5:205–208.

Kunzle H. 1975. Bilateral projections from precentral motor cortex to the putamen and other parts of the basal ganglia. An autoradiographic study in *Macaca fascicularis*. Brain Res 88:195–209.

Lapper SR, Bolam JP. 1992. Input from the frontal cortex and the parafascicular nucleus to cholinergic interneurons in the dorsal striatum of the rat. Neuroscience 51:533–545.

Lapper SR, Smith Y, Sadikot AF, Parent A, Bolam JP. 1992. Cortical input to parvalbumin-immunoreactive neurones in the putamen of the squirrel monkey. Brain Res 580:215–224.

Larsson E, Lindvall O, Kokaia Z. 2001. Stereological assessment of vulnerability of immunocytochemically identified striatal and hippocampal neurons after global cerebral ischemia in rats. Brain Res 913:117–132.

Lavdas AA, Grigoriou M, Pachnis V, Parnavelas JG. 1999. The medial ganglionic eminence gives rise to a population of early neurons in the developing cerebral cortex. J Neurosci 19:7881–7888.

Luk KC, Sadikot AF. 2001. GABA promotes survival but not proliferation of parvalbumin-immunoreactive interneurons in rodent neostriatum: an in vivo study with stereology. Neuroscience 104:93–103.

Luk KC, Kennedy TE, Sadikot AF. 2003. Glutamate promotes proliferation of striatal neuronal progenitors by an NMDA receptor-mediated mechanism. J Neurosci 23:2239–2250.

Marchand R, Lajoie L. 1986. Histogenesis of the striopallidal system in the rat. Neurogenesis of its neurons. Neuroscience 17:573–590.

Marin O, Anderson SA, Rubenstein JL. 2000. Origin and molecular specification of striatal interneurons. J Neurosci 20:6063–6076.

McGeorge AJ, Faull RL. 1989. The organization of the projection from the cerebral cortex to the striatum in the rat. Neuroscience 29:503–537.

Morrell MJ. 1999. Epilepsy in women: the science of why it is special. Neurology 53:S42–S48.

Nowakowski RS, Lewin SB, Miller MW. 1989. Bromodeoxyuridine immunohistochemical determination of the lengths of the cell cycle and the DNA-synthetic phase for an anatomically defined population. J Neurocytol 18:311–318.

Olsson M, Campbell K, Wictorin K, Bjorklund A. 1995. Projection neurons in fetal striatal transplants are predominantly derived from the lateral ganglionic eminence. Neuroscience 69:1169–1182.

Olsson M, Bjorklund A, Campbell K. 1998. Early specification of striatal projection neurons and interneuronal subtypes in the lateral and medial ganglionic eminence. Neuroscience 84:867–876.

Oorschot DE. 1996. Total number of neurons in the neostriatal, pallidal, subthalamic, and substantia nigral nuclei of the rat basal ganglia: a stereological study using the cavalieri and optical disector methods. J Comp Neurol 366:580–599.

Pakzaban P, Deacon TW, Burns LH, Isacson O. 1993. Increased proportion of acetylcholinesterase-rich zones and improved morphological integration in host striatum of fetal grafts derived from the lateral but not the medial ganglionic eminence. Exp Brain Res 97:13–22.

Parent A. 1996. The basal ganglia. In: Carpenter's human neuroanatomy. Baltimore: Williams & Wilkins. p. 795–863.

Paxinos G, Watson C. 1998. The rat brain in stereotaxic coordinates. New York: Academic Press.

Penny GR, Wilson CJ, Kitai ST. 1988. Relationship of the axonal and dendritic geometry of spiny projection neurons to the compartmental organization of the neostriatum. J Comp Neurol 269:275–289.

Phelps PE, Brady DR, Vaughn JE. 1989. The generation and differentiation of cholinergic neurons in rat caudate-putamen. Brain Res Dev Brain Res 46:47–60.

Rakic P. 1971. Guidance of neurons migrating to the fetal monkey neocortex. Brain Res 33:471–476.

Ramanathan S, Hanley JJ, Deniau JM, Bolam JP. 2002. Synaptic convergence of motor and somatosensory cortical afferents onto GABAergic interneurons in the rat striatum. J Neurosci 22:8158–8169.

Reich DL, Silvay G. 1989. Ketamine: an update on the first twenty-five years of clinical experience. Can J Anaesth 36:186–197.

Résibois A, Rogers JH. 1992. Calretinin in rat brain: an immunohistochemical study. Neuroscience 46:101–134.

Rudkin TM, Sadikot AF. 1999. Thalamic input to parvalbumin-immunoreactive GABAergic interneurons: organization in normal striatum and effect of neonatal decortication. Neuroscience 88:1165–1175.

Rushlow W, Naus CC, Flumerfelt BA. 1996. Somatostatin and the patch/matrix compartments of the rat caudate-putamen. J Comp Neurol 364:184–190.

Rymar VV, Sadikot AF. 2001. Neurogenesis of the calretinin-immunoreactive GABAergic interneurons of the forebrain. Presented at the 30th Annual Meeting of the Society for Neuroscience, San Diego, November 10–15. Abstract 359.10.

Rymar VV, Sadikot AF. 2002. Differential birthdate of calretinin-immunoreactive GABAergic interneurons in patch and matrix compartments of the rat striatum. Presented at the 31th Annual Meeting of the Society for Neuroscience, Orlando, November 2–7. Abstract 724.3.

Sadikot AF, Sasseville R. 1997. Neurogenesis in the mammalian neostriatum and nucleus accumbens: parvalbumin-immunoreactive GABAergic interneurons. J Comp Neurol 389:193–211.

Sadikot AF, Parent A, Francois C. 1992a. Efferent connections of the centromedian and parafascicular thalamic nuclei in the squirrel monkey: a PHA-L study of subcortical projections. J Comp Neurol 315:137–159.

Sadikot AF, Parent A, Smith Y, Bolam JP. 1992b. Efferent connections of the centromedian and parafascicular thalamic nuclei in the squirrel monkey: a light and electron microscopic study of the thalamostriatal projection in relation to striatal heterogeneity. J Comp Neurol 320: 228–242.

Sadikot AF, Rudkin T, Smith Y. 1996. The amygdalostriatal projection: an analysis of synaptic inputs to GABAergic interneuron subtypes. The basal ganglia—V. In: Ohye C, Kimura M, McKenzie JF, editors. Advances in behavioral biology. New York: Plenum Press. p 33–42.

Sadikot AF, Rymar VV, Mittal S, Luk KC. 2000. Neurogenesis of calretinin- and parvalbumin-immunoreactive GABAergic interneurons in the mammalian cerebral cortex. Presented at the 29th Annual Meeting of the Society for Neuroscience, New Orleans, November 4–9. Abstract 693.5.

Semba K, Vincent SR, Fibiger HC. 1988. Different times of origin of choline acetyltransferase- and somatostatin-immunoreactive neurons in the rat striatum. J Neurosci 8:3937–3944.

Sidibé M, Smith Y. 1999. Thalamic inputs to striatal interneurons in monkeys: synaptic organization and co-localization of calcium binding proteins. Neuroscience 89:1189–1208.

Smart IHM, Sturrock RR. 1979. Ontogeny of the neostriatum. In: Divak I, Öberg RGE, editors. The neostriatum. New York: Pergamon. p 127–146.

Smith Y, Parent A. 1986. Differential connections of caudate nucleus and putamen in the squirrel monkey (*Saimiri sciureus*). Neuroscience 18: 347–371.

Somogyi P, Smith AD. 1979. Projection of neostriatal spiny neurons to the substantia nigra. Application of a combined Golgi-staining and horseradish peroxidase transport procedure at both light and electron microscopic levels. Brain Res 178:3–15.

Song DD, Harlan RE. 1994. Genesis and migration patterns of neurons forming the patch and matrix compartments of the rat striatum. Brain Res Dev Brain Res 83:233–245.

Soriano E, Del Rio JA. 1991. Simultaneous immunocytochemical visualization of bromodeoxyuridine and neural tissue antigens. J Histochem Cytochem 39:255–263.

Sussel L, Marin O, Kimura S, Rubenstein JL. 1999. Loss of Nkx2.1 homeobox gene function results in a ventral to dorsal molecular respecification within the basal telencephalon: evidence for a transformation of the pallidum into the striatum. Development 126:3359–3370.

Tabakoff B, Rabe CS, Hoffman PL. 1991. Selective effects of sedative/hypnotic drugs on excitatory amino acid receptors in brain. Ann N Y Acad Sci 625:488–495.

Tamamaki N, Fujimori KE, Takauji R. 1997. Origin and route of tangentially migrating neurons in the developing neocortical intermediate zone. J Neurosci 17:8313–8323.

ten Donkelaar HJ, Dederen PJ. 1979. Neurogenesis in the basal forebrain of the Chinese hamster (*Cricetulus griseus*). I. Time of neuron origin. Anat Embryol 156:331–348.

Tennyson VM, Barrett RE, Cohen G, Cote L, Heikkila R, Mytilineou C. 1972. The developing neostriatum of the rabbit: correlation of fluorescence histochemistry, electron microscopy, endogenous dopamine levels, and (^{3}H)dopamine uptake. Brain Res 46:251–285.

Toresson H, Campbell K. 2001. A role for Gsh1 in the developing striatum and olfactory bulb of Gsh2 mutant mice. Development 128:4769–4780.

van der Kooy D, Fishell G. 1987. Neuronal birthdate underlies the development of striatal compartments. Brain Res 401:155–161.

van Vulpen EHS, van der Kooy D. 1996. Differential maturation of cholinergic interneurons in the striatal patch vs. matrix compartments. J Comp Neurol 365:683–691.

van Vulpen EHS, van der Kooy D. 1998. Striatal cholinergic interneurons: birthdates predict compartmental localization. Brain Res Dev Brain Res 109:51–58.

Vincent SR, Johansson O. 1983. Striatal neurons containing both somatostatin- and avian pancreatic polypeptide (APP)-like immunoreactivities and NADPH-diaphorase activity: a light and electron microscopic study. J Comp Neurol 217:264–270.

Webster KE. 1961. Cortico-striate interrelations in the albino rats. J Anat 95:532–544.

West MJ, Ostergaard K, Andreassen OA, Finsen B. 1996. Estimation of the number of somatostatin neurons in the striatum: an in situ hybridization study using the optical fractionator method. J Comp Neurol 370: 11–22.

Wichterle H, Garcia-Verdugo JM, Herrera DG, Alvarez-Buylla A. 1999. Young neurons from medial ganglionic eminence disperse in adult and embryonic brain. Nat Neurosci 2:461–466.

Wu Y, Parent A. 2000. Striatal interneurons expressing calretinin, parvalbumin or NADPH-diaphorase: a comparative study in the rat, monkey and human. Brain Res 863:182–191.

Yeterian EH, Van Hoesen GW. 1978. Cortico-striate projections in the rhesus monkey: the organization of certain cortico-caudate connections. Brain Res 139:43–63.

Zhu Y, Li H, Zhou L, Wu JY, Rao Y. 1999. Cellular and molecular guidance of GABAergic neuronal migration from an extracortical origin to the neocortex. Neuron 23:473–485.